1. Pyroelectricty- What is it and what is it for

Pyroelectricity is a phenomenon known from ancient times, when it was first described in 314 BC by the greek philosopher Theophrastus in his treatise "On Stones".[1.] He noted that the stone lyngourion (most probably the mineral tourmaline) becomes charged when heated thus attracting bits of sawdust or straw. In the beginning of the 18th century J. G. Schmidt described the experience of Dutch gem cutters that tourmaline had the property of not only attracting the ashes from the warm or burning coals, as a magnet does iron, but also of repelling them again by and by.[2] These two observations already describe the basic behavior of pyroelectric materials when responding to heat flow[3]- charge generation upon temperature change followed by gradual charge disappearance, if the temperature stays at a constant level.

In a rigorous definition we understand pyroelectricity as the temperature dependence of the spontaneous polarization P_S in the crystal, with P_S representing the dipole moment per unit volume of the material. The pyroelectric coefficient p is defined as

$$p = \frac{dP_s}{dT}\bigg|_{E,S} \tag{1}$$

(under constant elastic stress S and constant electric field E) and it relates a change in temperature T to a change in electrical displacement D according to the relation, $dD = p \cdot dT$. Thus the material becomes polarized under temperature changes resulting in the generation of a charge Q on the surface area A that may attract free charges from the environment (ions, electrons, dust, ...) or, when electrodes are attached to this surface, may be measured as a current (the pyroelectric current I_p) generated to compensate the T-induced polarization charges (see Fig. 1a). To pick up the charge dQ that is generated by the temperature change dT, the pyroelectric materials are fabricated typically in the shapes of a flat capacitor with area A with two electrodes on opposite sides and the pyroelectric material serving as a dielectric (see Fig. 1a). The generated charge and the pyroelectric current I_p (under short-circuit conditions) are then given by the equations

$$dQ = p \cdot A \cdot dT \tag{2}$$

$$I_p = p \cdot A \cdot \frac{dT}{dt} \tag{3}$$

Here p is the pyroelectric coefficient that results from the sum of the crystalline or molecular dipole moments oriented normal to the electrodes.

Two contributions make up the pyroelectric effect.[4] The primary pyroelectric effect refers to a clamped crystal (meaning constant strain) for which a change in temperature induces directly a change in electric displacement (due to the elongation or shortening of individual dipoles), also known as the dimensional change, whereas the secondary pyroelectric effect is a result of crystal deformation and is mediated by the piezoelectric effect – the thermal expansion or contraction causes a strain in the crystal that alters the electric displacement due to its piezoelectricity, which is also known as electrostriction. The temperature dependent libration of dipoles may also contribute to the secondary effect, especially in polymer pyroelectric materials. The sum of these effects, the so-called total pyroelectric effect under constant stress, is what is usually measured as p.

The most important application of the pyroelectric effect is the detection of long-wavelength infrared radiation, especially in the range from 8 to 14 μm, [5,6,7,8,10] which covers the peak in emission of the black-body curve for objects at 300 K (that occurs at 10 μm). Consequently, IR

detectors with high sensitivity at a wavelength of 10 μm can easily detect human beings and other warm-blooded animals. Thermal detectors that convert heat into photons like pyroelectric detectors are cheap in manufacture, have a large spectral bandwidth and are sensitive over a wide temperature range. However, since they only react on temperature fluctuations, they are used mainly to detect moving objects in a scene or stationary objects through a light chopper. Some of the applications of IR pyroelectric detectors include intruder alarms[6] and motion detectors[9] for building protection, light control switches,[10] radiometers,[6] instant medical IR thermometers,[3] flame and fire detectors,[6] IR spectrometers,[14] laser power meters,[10] pollution monitors[6] and thermal imaging systems (vidicons or point detector arrays).[6,11,12] Apart from IR detection the pyroelectric effect has also been exploited for electron-emission devices or the characterization of thermal and optical properties of materials.[14]
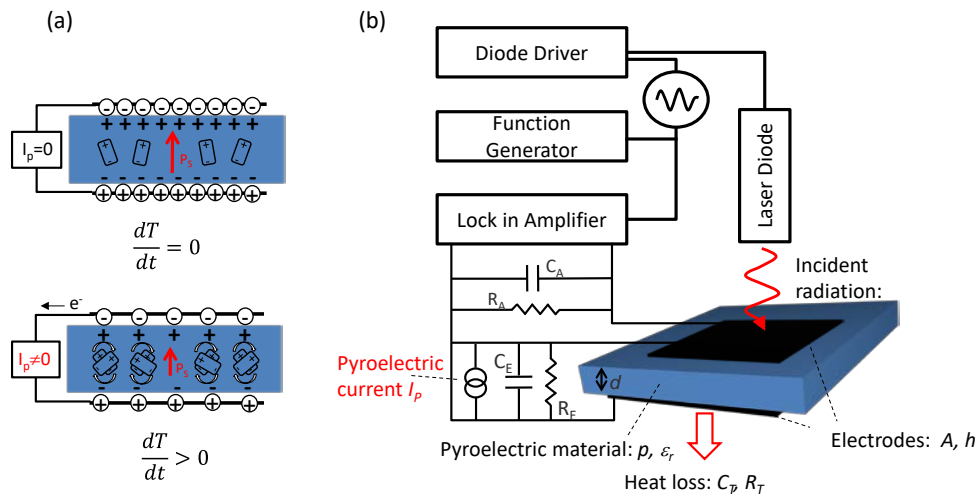

Figure 1: (a) Scheme illustrating the pyroelectric effect for a material with a given spontaneous polarization P_S (drawn in blue) made up of individual dipoles (crystallites, domains) sandwiched between electrodes (drawn in black). For a constant temperature and thus constant P_S the bound charges at the surface of the material are compensated by accumulated charges at the electrodes. For an increasing temperature P_S is prompted to decrease as the dipole moments, on average, diminish in magnitude. This decrease of P_S is pictured in the lower image by the horizontal tilting of the dipoles together with an increased libration amplitude. A current flows from the electrodes o compensate for the change in bound charge that accumulates on the crystal edges.

2. Theory of pyroelectric IR detector response

The response of pyroelectric IR detectors can be described in a very simple way by accounting for the analogy of thermal and electrical quantities and laws.[4-6,13] Let us assume a pyroelectric detector in the form of a parallel plate capacitor that is geometrically characterized by the thickness d of the pyroelectric dielectric layer sandwiched between electrodes of area A and emissivity η. Thermally, this detector is specified by the specific heat capacity C_T and the thermal resistance R_T, both forming the thermal time constant $\tau_T = R_T \cdot C_T$. Electrically the element itself can be described by the electrical capacitance C_E and the electrical resistance R_E. However, in any practical measurement setup an electrical readout circuit, characterized by resistance R_A and capacitance C_A, will be connected in parallel to the detector and therefore the overall electrical resistance R of the equivalent circuit reads as $R = \left(\frac{1}{R_A} + \frac{1}{R_E}\right)^{-1}$ and its overall electrical capacitance C as $C = C_A + C_E$, which both then constitute the electrical time constant $\tau = R \cdot C$.

The incoming IR radiation power $W(t) = W_o \cdot e^{i\omega t}$ (characterized by the modulation frequency ω) induces a heat transfer rate (heat current)

$$\dot{Q} = \eta W(t) = \frac{\vartheta}{R_T} + C_T \cdot \frac{d\vartheta}{dt} \tag{3}$$

, with ϑ being the temperature difference to the ambient that is generated in the pyroelectric element by the modulated IR radiation. Here the heat transfer rate $\dot{Q}$ is seen as an equivalent to the electrical current $I = \dot{q}$ (with electrical charge q) and thus Equ. (3) describes the thermal "charging" current of the $R_T C_T$-element as an equivalent to the electrical charging current of the RC-element. ϑ is an analogue to the electrical potential difference or voltage V.

Solving differential equation (3) reads as

$$\vartheta = \frac{R_T \cdot \eta W_0}{(1 + i\omega\tau_T)} \cdot e^{i\omega t} \tag{4}$$

From this the pyroelectric current responsivity R_I, which is the absolute value of pyroelectric current I_P per Watt of input power, is described as

$$R_I = \frac{|I_P|}{|W|} = \frac{pA}{W_0} \cdot \left|\frac{d\vartheta}{dt}\right| = \frac{\eta pA \cdot R_T \cdot \omega}{\sqrt{1 + \omega^2 \tau_T^2}} \tag{5}$$

For low frequencies ($\omega \gg 1/\tau_t$) R_I increases proportional to the frequency, whereas for high frequencies with $\omega \gg 1/\tau_t$ the current responsivity is constant according to

$$R_I^{HF} = \frac{\eta pA}{C_T} = \frac{\eta p}{C_T' \cdot d} \tag{6}$$

Here $C_T' = C_T/(d \cdot A)$ is the volumetric heat capacity.

The voltage responsivity R_V, which is the pyroelectric voltage per Watt of incident radiation power, is derived from the pyroelectric current or, more precisely, from R_I by dividing it with the absolute value of the admittance $Y = R^{-1} + i\omega C$ of an RC-element

$$R_V = \frac{|I_p|}{|W|} \cdot \frac{1}{|Y|} = R_I \cdot \frac{1}{|Y|} = \frac{\eta pA \cdot R_T \cdot \omega}{\sqrt{1 + \omega^2 \tau_T^2}} \cdot \frac{R}{\sqrt{1 + \omega^2 \tau^2}} \tag{8}$$

For very low frequencies ($\omega \ll 1/\tau_t$ and $\omega \ll 1/\tau$) the voltage responsivity increases with ω, whereas it decreases with $1/\omega$ for high frequencies ($\omega \gg 1/\tau_t$ and $\omega \gg 1/\tau$) according to

$$R_V^{HF} = \frac{\eta p}{C_T' \cdot d} \cdot \frac{1}{C \cdot \omega} \tag{9}$$

, thus R_V develops a maximum in the frequency range between $1/\tau_T$ and $1/\tau$ (very often the thermal time constant is larger than the electrical one). For minimal capacitance of the read-out circuit C_A, $C \sim C_E = \varepsilon_r \varepsilon_0 \cdot A/d$ and then a constant for the pyroelectric material can be defined, namely the voltage figure-of-merit (FOM) F_V, that is independent of any geometry parameter and electrode emissivity. The high frequency limit of the voltage responsivity then corresponds to

$$R_V = \frac{\eta F_V}{A \cdot \omega} \quad \text{with} \quad F_V = \frac{p}{C_T' \cdot \epsilon_r \epsilon_0} \tag{10}$$

3. Pyroelectric materials for high resolution IR detectors.

Pyroelectricity occurs in certain (semi)crystalline materials that have to fulfil three conditions:[14] The molecular structure must have a nonzero dipole moment; the material must not have center of symmetry; and the material must have either no or a single axis of rotational symmetry that is not included in an inversion axis. Of the 32 crystal classes, 21 are non-centrosymmetric, and 10 of these exhibit pyroelectric properties. Besides pyroelectric properties, all these materials exhibit some degree of piezoelectric properties as well—they generate an electric charge in response to mechanical stress. Some of the pyroelectric materials are ferroelectric, meaning that the spontaneous electrical polarization can be reversed by a sufficiently strong external electric field and that the material is characterized by the Curie temperature, T_c, above which it is paramagnetic. These materials are either inorganic ceramics like $BaTiO_3$[15] or crystals like Triglycerine sulfate[14,16] and $LiNbO_3$[17], semi-crystalline polymers like PVDF (Polyvinylidene fluoride)[18,19,20] and its copolymer with TrFE (Trifluoroethylene)[21,22] or even biological materials like collagen and peptides[23,24] or hydroxyapatite[25], a major component of bone. Ferroelectric materials generally exhibit larger pyroelectric coefficients than non-ferroelectrics and therefore are of greater interest for applications (see Table 1).

Ferroelectric ceramics as well as semi-crystalline polymers are composed of a large number of crystallites which, after fabrication, are typically randomly oriented. Accordingly, the crystalline dipole moments are also randomly oriented and will not deliver a measurable spontaneous polarization. To maximize P_S and thus activate the pyroelectric effect, it is necessary to apply a sufficiently large electric field E (larger than the coercive field and, optionally, at elevated temperature and time) across the ferroelectric material in order to align the polar axis of the crystallites as near to the direction of the external poling field as the crystal structure and its local environment will allow. This procedure is called poling and it can be done in a DC field, in an AC field during a hysteresis loop measurement or by Corona discharge, either uniform or in a patterned way.[26]

Apart from the pyroelectric coefficient p, Table 1 also lists the relative permittivity ε_r and the FOM F_V, which can be used to compare different pyroelectric materials for their potential as IR detectors irrespective of electrode area and emissivity.[6] F_V only contains parameters describing the properties of the pyroelectric material and is the higher, the higher is p and the lower is ε_r (see Eq. 10). If, as is often the case in real world applications, the pyroelectric material is mounted directly on a substrate with a good heat conductivity thus forming a heat sink (such as an integrated silicon circuit) then another voltage FOM, $F_{V,sink}$, comes into play.[27,28] $F_{V,sink}$ also accounts for the thermal conductivity of the pyroelectric material and is the higher, the higher is the pyroelectric coefficient and the lower are both the thermal conductivity and the permittivity. The lateral thermal resolution $1/l$ [ii] of a free standing pyroelectric material, also listed in Table 1, is mainly determined by its thermal conductivity λ.[12] For the calculation of $1/l$ a thickness d = 10 µm and a heat transfer coefficient into air $\alpha \sim 11$ WK/m² (measured value taken from Ref. 12) for all the indicated materials were assumed.

Table 1: Different types of pyroelectric materials with their pyroelectric coefficient p (at an ambient temperature of 25°C), the pyroelectric voltage FOM (figure-of-merit) F_V, the pyroelectric voltage FOM with heat sink $F_{V,sink}$[i], the relative permittivity ε_r, the thermal conductivity λ and the lateral resolution $1/l$ [ii] of a free standing material with thickness d =10 μm and α = 11 W/Km^2.[12,29] The material parameters p, λ and ε_r are taken from the references indicated. The record values (largest p, F_V, $F_{V,sink}$ and 1/l as well as smallest ε_r and λ) are printed in bold.

Material	p [μC/m²K]	F$_V$ [10⁻³m²/C]	F$_{V,sink}$ [10⁶V/W]	ε_r	λ [W/mK]	1/l [μm⁻¹]
Ferroelectric ceramics						
$PbZr_{0.5}Ti_{0.5}O_3$ or PZT[12]	-420	11	25	1600	1.2	1.35
$PbZr_{0.3}Ti_{0.7}O_3$[30,31]	-400	28	68	558	1.2	1.35
$BaTiO_3$[12]	-400	15	15	1000	3.0	0.86
$PbTiO_3$[32]	-250	46	74	190	2.0	1.05
Ferroelectric crystals						
$Sr_{0.5}Ba_{0.5}Nb_2O_6$[6,33]	**-550**	66	151	400	1.0	1.46
$Ca_{0.15}(Sr_{0.5}Ba_{0.5})_{0.85}Nb_2O_6$[34,35]	-360	21	36	933	1.2	1.35
Triglycerine sulfate or TGS[14,12]	-350	**527**	3294	30	0.4	2.35
$LiTaO_3$ or lithium tantalate[12]	-200	157	120	45	4.2	0.72
$Pb_5Ge_3O_{11}$ or lead germanate[14,36]	-110	173	531	30	0.8	1.68
$Ca_{10}(PO_4)_6(OH)_2$ or Hydroxyapatite[25]	-12	24	36	25	0.15	3.83
Ferroelectric semicrystalline polymers						
$(CH_2CF_2)_n$ or PVDF[14,21]	-27	147	2420	9	**0.13**	**3.96**
P(VDF-TrFE) w. 20 % TrFE [14,22,37,7]	-31	217	**3573**	**7**		
P(VDF-TrFE) w. 50 % TrFE [39,22]	-52	114	1793	18		
$P(VDF\text{-}TrFE)_{0.5}:(PZT)_{0.5}$[38,39]	-45	27	141	72	0.5	2.10
$P(VDF\text{-}TrFE)_{0.7}:(PZT)_{0.3}$[38,39,40]	-92	80	462	45		
Non-Ferroelectric crystals						
CdSe[14]	-3.5	7	4,4	10	9.0	0.49
CdS[14]	-4.0	13	1,3	8.9	40.1	0.23
ZnO[14]	-9.4	66	1,1	8.5	110.0	0.14
Tourmaline[14]	-4.0	-	-	25	-	-

According to Table 1, **TGS** and its isomorphs have very high pyroelectric coefficients (p ~ -350 μC/m²K) and, due to their low permittivity, also very large voltage FOMs (F_V ~ 0.5 m²/C and $F_{V,sink}$ ~ 3300 kV/W); however, they are not very stable due to their tendency to absorb (and even dissolve in) water and their mechanical brittleness. In addition, the Curie temperature T_c of TGS is very low (49°C) thus strongly limiting its applicability. It was discovered that doping of TGS crystals with l-alanine during its growth (LATGS process patented by Philips) stabilizes the material below the Curie temperature (that was raised to 60 °C).[41] This allows its use as high-sensitive IR radiation detector at the upper operating temperature of 55 °C which is sufficient for many applications (single element detectors, vidicons).[16]

LiTaO₃ has a comparably high pyroelectric coefficient p ~ -200 μC/m²K, reasonably large FOMs (F_V ~ 0.16 m²/C and $F_{V,sink}$ ~ 120 kV/W), is insensitive to humidity and has a high Curie temperature (> 600°C) and melting point. Therefore it is more attractive than **lead germanate**,

---

[i] $F_{V,sink} = -\frac{p}{\lambda \cdot \varepsilon_r \varepsilon_0}$, with pyroelectric coefficient p, thermal conductivity λ and relative permittivity ε_r, $R_A \ll R_E$ [28]

[ii] $\frac{1}{l} = \sqrt{\frac{2\alpha}{\lambda \cdot d}}$ with the thermal conductivity λ, the thickness d and the heat transfer coefficient α.[12]

which has larger FOMs ($F_V \sim 0.17$ m^2/C and $F_{V,sink} \sim 530$ kV/W) but a rather low T$_c$ of 180 °C or the **niobates,** which have high pyroelectric coefficients but also high permittivity values, thus resulting in rather low FOMs. These factors make LiTaO$_3$ one of the most stable pyroelectrics with a very wide temperature range of operation useable also in space applications.[14]

In order to maximize the pyroelectric voltage responsivity it is necessary to minimize the thermal mass of the pyroelectric material, which is typically achieved by decreasing its thickness and its thermal conductivity. For single crystal pyroelectrics decreasing the thickness is a complicate and costly process, including cleaving and polishing, which limits the achievable detector area. Ceramic perovskite pyroelectric materials like **PbTiO$_3$** or **PZT** are easier to manufacture as thin films (e.g. by sol-gel spin casting [42]), however they typically have very high dielectric constants and high thermal conductivity which limits the pyroelectric voltage FOMs ($F_V < 0.05$ m^2/C and $F_{V,sink} < 70$ kV/W).

Although the semi-crystalline polymer **PVDF** and its copolymer **PVDF-TrFE** (VDF:TrFE ratio varying between 50:50 and 80:20) have comparably low pyroelectric coefficients ($p \sim$-25 to -40 µC/m^{2}K)[22,7] as compared to ceramics and crystals, their low dielectric constants result in very high FOM values ($F_V \sim$ 0.1-0.2 m^2/C and $F_{V,sink} < 3500$ kV/W). The low thermal conductivity of these polymers in particular implies a high lateral resolution and small signal crosstalk which recommends them as pyroelectric materials for large-area detectors and thermal imaging arrays.
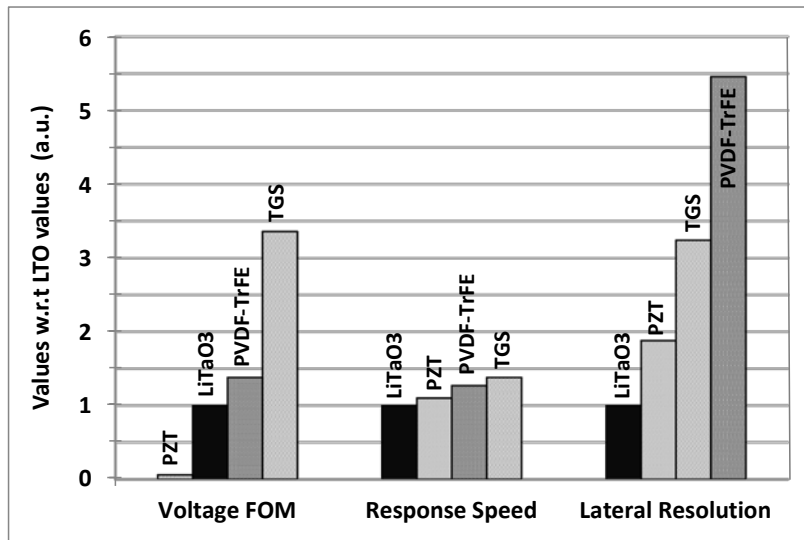

Figure 2: Principal sensor properties (voltage FOM F_V, response speed v_{th} and lateral resolution l^{-1}) of various free-standing pyroelectric materials normalized to the respective values of LiTaO$_3$ of identical thickness.

In Figure 1 the principal sensor properties of the most important pyroelectric materials are compared, which are the pyroelectric voltage FOM F_V, the response speed v_{th}[iii] and the lateral resolution $1/l$. The thickness of all materials was assumed to be identical and the heat transfer coefficient into air $\alpha \sim 11$ W/Km^2 was taken from Ref. 12. It is obvious that PVDF-TrFE has very good sensor properties; it is superior in terms of spatial resolution of the thermal signal, which is mainly due to its comparably low thermal conductivity and it is very fast and delivers large voltage signals. If the PVDF copolymer sensor is mounted on a substrate with high thermal

---

[iii] $v_{th} = \frac{c'}{2\alpha \cdot d}$ with α being the heat transfer coefficient into air, c' being the volumetric specific heat and d being the thickness of the material .[12]

conductivity (e.g. a silicon integrated circuit for sensor readout) its generated voltage signal ($\sim F_{V,sink}$) is even higher than that one of a TGS sensor with identical geometry.

Pyroelectric IR detectors implemented on the basis of single crystals such as TGS or $LaTiO_3$ and PZT ceramics often impose problems in handling and preparing brittle crystals or ceramics with thicknesses below 30 μm, in realizing thermally and acoustically insulated mounting and in applying metallization for the crystals, problems which are not encountered with ferroelectric polymers. Out of processing alone the use of PVDF-based sensors is also attractive due to its excellent FOM value (140% of that one of $LiTaO_3$, still the most commonly used material) and the possibility to increase speed by up to a factor of 5 by reducing the film thickness to below 10 μm. Another advantage is the high lateral thermal resistance which allows the use of a self-supporting substrate extending beyond the edge of the pyroelectric film and a substantial increase in resolution.

[1] E. R. Caley, J. F. C. Richards, *Theophrastus On Stones*, Graduate School Monographs, Contributions in Physical Science No.1, The Ohio State University 1956

[2] J. G. Schmidt, *Curiöse Speculationes bey Schlaflosen Nächten,* Chemnitz und Leipzig: Conrad Stöffel, 1707.

[3] J. Fraden, *Handbook of Modern Sensors*, 4th edn. New York: Springer Verlag, 2010.

[4] S. B. Lang, Sourcebook of Pyroelectricity, Gordon & Breach Science, London (1974)

[5] P. Muralt, *Micromachined infrared detectors based on pyroelectric thin films*, Rep. Prog. Phys. 64, 1339 (2001).

[6] R. W. Whatmore, *Pyroelectric devices and materials*, Rep. Prog. Phys. **49**, 1335 (1986).

[7] S. B. Lang, D. K. Das-Gupta, *Pyroelectricity: fundamentals and applications* in *Handbook of Advanced Electronic and Photonic Materials and Devices*, vol. 4, H. S. Nalwa, ed., Academic Press, San Diego, CA (2001)

[8] M. H. Lee, R. Guo, A. S. Bhalla, J. Electroceram. **2**, 229 (1998)

[9] Sensitec AG, sensitec@sensitec-ag.ch (1.11. 2016)

[10] J. Fraden, *Pyroelectric Detectors* , Chap. 73 in Measurement, instrumentation and sensors handbook: ed. by J. G. Webster and H. Eren, CRC Press Taylor&Francis, Boca Raton-London-New York (2014)

[11] H. Meixner, G. Mader, and P. Kleinschmidt, *Infrared sensors based on the pyroelectric polymer polyvinylidene fluoride (PVDF)*, Siemens Forsch. Entwickl. Ber., 15(3), 105–114, 1986

[12] H. Meixner, *IR-sensor-arrays based on PVDF*, Ferroelectrics 115, 279 (1991)

[13] J. Cooper, *Minimum Detectable Power of a Pyroelectric Thermal Receiver,* Rev. Sci. Instrum. 33, 92 (1962)

[14] S. B. Lang, *Pyroelectricity: From Ancient Curiosity to Modern Imaging Tool*, Physics Today, August 2005, p.31.

[15] B. Ertuğ, *The Overview of The Electrical Properties of Barium Titanate*, Am. J. Eng.Res. **2**, 1 (2013)

[16] M.D. Aggarwal, A.K. Batra, P. Guggilla, and M.E. Edwards, B.G. Penn and J.R. Currie, Jr., *Pyroelectric Materials for Uncooled Infrared Detectors: Processing, Properties, and Applications*, https://www2.sti.nasa.gov (2010)

[17] S. T. Popescu, A. Petris, and V. I. Vlad, Interferometric measurement of the pyroelectric coefficient in lithium niobate, J. Appl. Phys. 113, 043101 (2013)

[18] The piezoelectricity of PVDF was first reported by H. Kawai in The piezoelectricity of poly(vinylidene fluoride), Jpn. J. Appl. Phys. 8, 875 (1969)

[19] The pyroelectricity of PVDF was first described by J. G. Bergman, J. H. McFee, and G. R. Crane in *Pyroelectricity and optical second harmonic generation in polyvinylidene fluoride films*, Appl. Phys. Lett. 18 , 203 (1971)

[20] R. G. Kepler, *Piezo electricity, pyroelectricity, and ferroelectricity in organic materials*, Ann. Rev. Phys. Chem. 29, 497 (1978)

[21] D. K. Das-Gupta, *Pyroelectricity in polymers*, Ferroelectrics 118, 165 (1991)

[22] T. Furukawa, Piezoelectricity and Pyroelectricity in Polymers, IEEE Transactions on Electrical Insulation 24, 375 (1989)

[23] S. B. Lang, *Pyroelectric effect in bone and tendon*, Nature 212, 704–705 (1966)

[24] S.B. Lang, A. A. Marino, G. Berkovic, M. Fowler, K. D. Abreo, *Piezoelectricity in the human pineal gland*, Bioelectrochem. Bioenerg. 41, 191–195 (1996).

[25] S. B. Lang, S. A. M. Tofail, A. A. Gandhi, M. Gregor, C. Wolf-Brandstetter, J. Kost, S. Bauer, and M. Krause, *Pyroelectric, piezoelectric, and photoeffects in hydroxyapatite thin films on silicon*, Appl. Phys. Lett. 98, 123703 (2011)

[26] Y. Qiu, *Patterned piezo-, pyro-, and ferroelectricity of poled polymer electrets*, J. Appl. Phys. 108, 011101 (2010)

[27] S. Bauer, S. Bauer-Gogonea, B. Ploss, *The physics of pyroelectric infrared devices*, Appl. Phys. B 54, 544 (1992)

[28] B. Ploss, S. Bauer, *Characterization of materials for integrated pyroelectric sensors*, Sensors and Actuators A, 25-27, 407-411 (1991)

[29] http://www.schweizer-fn.de/waerme/waermeuebergang/waerme_uebergang.php

[30] W. Liu, J. S. Ko, W. Zhu, *Preparation and properties of multilayer $Pb(Zr,Ti)O_3/PbTiO_3$ thin films for pyroelectric application*, Thin Solid Films 371, 254 (2000)

[31] M. T. Kesim, J. Zhang, S. Trolier-McKinstry, J. V. Mantese, R. W. Whatmore, and S. P. Alpay, *Pyroelectric response of lead zirconate titanate thin films on silicon: Effect of thermal stresses*, J. Appl. Phys. 114, 204101 (2013)

[32] R. Takayama, Y. Tomita, K, lijima and I. Ueda, Ferroelectrics 118, 325 (1991).

[33] C. S. Dandeneau, T. W. Bodick, R. K. Bordia, and F. S. Ohuchi, *Thermoelectric Properties of Reduced Polycrystalline $Sr_{0.5}Ba_{0.5}Nb_2O_6$ Fabricated Via Solution Combustion Synthesis*, J. Am. Chem. Soc. 96, 2230 (2013)

[34] J. Zhang, X. Dong, F. Cao, S. Guo, and G. Wang, *Enhanced pyroelectric properties of $Ca_x(Sr_{0.5}Ba_{0.5})_{1-x}Nb_2O_6$ lead-free ceramics*, Appl. Phys. Lett. 102, 102908 (2013)

[35] A. Speghini, M. Bettinelli, U. Caldino, M. O. Ramirez, D. Jaque, L. E. Bausa2 and J. Garcia Sole, *Phase transition in $Sr_xBa_{1-x}Nb2O6$ ferroelectric crystals probed by Raman spectroscopy,* J. Phys. D: Appl. Phys. **39** , 4930 (2006)

[36] X. Wu, J. Xu, W. Jin, *Thermal properties of lead germanate single crystals grown by the vertical Bridgman method*, J. Cryst. Growth 282, 160 (2005)

[37] B. Ploss, *Pyroelectric and nonlinear dielectric properties of copolymers of PVDF-TrFE* in <u>Handbook of Low and High Dielectric Constant Materials and Their Applications</u> : ed. by H. S. Nalwa, Academic Press 1999

[38] M. Dietze, M. Es-Souni, *Structural and functional properties of screen-printed PZT–PVDF-TrFE composites*, Sensors and Actuators A 143,329 (2008)

[39] M. Dietze, J. Krause, C.-H. Solterbeck, and M. Es-Souni, *Thick film polymer-ceramic composites for pyroelectric applications*; J. Appl. Phys. 101, 054113 (2007)

[40] C.-G. Wu, G.-Q. Cai, W.-B. Luo, Q.-X. Peng, X.-Y. Sun and W.-L. Zhang, *Enhanced pyroelectric properties of PZT/PVDF-TrFE composites using calcined PZT ceramic powders*, J. Adv. Dielect. 3, 1350004 (2013)

[41] Semiconductor Sensors, *Data Handbook*. Eindhoven, the Netherlands: Philips Export B.V., 1988.

[42] C. Ye, T. Tamagawa, and D.L. Polla, *Pyroelectric $PbTiO_3$ thin films for microsensor applications.* In: <u>Transducers'91. International Conference on Solid-State Sensors and Actuators,</u> San Francisco, CA, 904 (1991)